Laminar Dispersion in Jeffery-Hamel Flows: Part I. Diverging Channels

WILLIAM N. GILL and ÜLKÜ GÜCERI

Clarkson College of Technology, Potsdam, New York

Dispersion in flow in diverging channels, where the velocity decreases with axial distance is studied. Numerical experiments indicate:

1. At sufficiently large values of the angle of divergence and Peclet number, both axial and transverse molecular diffusion play minor roles in the dispersion process, and the system is dominated by convection. This is in marked contrast to parallel wall systems.

2. A dispersion model, given by Equation (15), is shown to exist for such flows for limited ranges of the Peclet number and angle of divergence.

3. At sufficiently large values of dimensionless time, the dependence of concentration on both axial position and time can be represented by a single similarity coordinate. This behavior is predicted by both the numerical solutions of Equation (3) and analytical solutions of the dispersion model.

G. I. Taylor (*23*, *24*) first described the rather complex process of dispersion, or miscible displacement, between flowing streams in tandem by a remarkably simple approximate theory which enabled him to calculate the dispersion coefficient from first principles. Aris (*2*) later confirmed Taylor's result by an alternate method and showed further that axial molecular diffusion contributes to the dispersion process in a linear, additive fashion. Carrier (*7*) analyzed the same problem by using still another method. Subsequently, Bailey and Gogarty (*5*) solved this problem by a finite difference technique. Aris, using the method of moments, generalized his earlier analysis to include time dependent flow (*4*) and multiphase systems (*3*).

Ananthakrishnan et al. (*1*) determined the regions of applicability of the dispersion model and the pure convection solution, where one neglects molecular diffusion altogether. Gill and Ananthakrishnan (*10*) gave consideration to the effect of inlet boundary conditions and stagnant pockets on the dispersion process. Subsequently, Gill (*12* to *14*) introduced a new analytical method of solving dispersion problems which enables one to consider multiphase systems with time variable flow in a relatively simple manner. Dispersion in three-dimensional velocity fields was discussed by Gill and Ananthakrishnan (*11*), Erdogan and Chatwin (*9*), and Nunge et al. (*18a*). Very recently Gill and Sankarasubramanian have developed an exact solution for all values of time for laminar dispersion in circular tubes (*14a*).

Experimental work on dispersion has been reported by a number of workers. Taylor (*23*) originally substantiated his analysis by comparing his theory with liquid-phase experiments. Bournia, Coull, and Houghton (*6*) conducted gas-phase experiments and found considerable differences between predicted and observed values of the dispersion coefficient in their slower flow experiments. These discrepancies were explained by Reejsinghani et al. (*20*) in terms of buoyancy effects, and these authors conducted liquid-phase experiments in horizontal tubes. In another paper, Reejsinghani et al. (*21*) did experiments on dispersion in vertical tubes and found that buoyancy forces can markedly influence dispersion even when very small differences in density are involved.

Dispersion in porous media has many practical implications, and it is clear that the flow in the interstices of such systems experiences local accelerations and decelerations because of changes in cross-sectional area. All previous work has been concerned with dispersion in flows in constant cross-sectional area conduits with parallel boundaries. Consequently, the present study was undertaken to determine if dispersion in systems with nonparallel boundaries differs significantly from dispersion in flows bounded by parallel walls. To this end, dispersion in Jeffery-Hamel flows between nonparallel diverging plates is studied, and it is found that even very small angles of divergence can markedly affect the dispersion process. This is particularly important when the Peclet number is large. In this event, the dispersion process may be dominated by convective effects to the extent that even for large values of dimensionless time τ, molecular diffusion, both parallel and perpendicular to the direction of flow, has a negligible effect on the average concentration distribution. In parallel plate systems, the effect of Peclet number is negligible for $N_{Pe} > 100$; however, in nonparallel plate systems, it appears that no such limiting value exists.

ANALYSIS

Fully Developed Viscous Flow in Converging and Diverging Passages

It is well known that viscous flow between two parallel plane walls is governed by a parabolic velocity distribution. In the case where the walls either converge or diverge, different velocity profiles can exist, depending on the value of the Reynolds number and the angle of convergence or diver-

gence of the system. The exact solutions of the Navier Stokes equations for these profiles were first obtained by Jeffery (*17*) in terms of elliptic functions, and later others (*8, 15, 18, 22*) extended his work. Goldstein (*15*) and later Rosenhead (*22*) gave an overall picture of the change in flow associated with increasing Reynolds number.

Millsaps and Pohlhausen (*18*) also obtained the mathematical expressions for different velocity profiles, and they analyzed the flows in diverging and converging channels separately. The exact velocity distribution profile for stable, fully developed flow in diverging channels can be written in terms of Jacobian elliptic functions which can be simplified considerably for small Reynolds numbers and angles of divergence. Their results for low Reynolds number flows in channels with small angles of divergence are

$$U = \nu \frac{F(\theta)}{r} = U_0 (1 - \theta^2) = \frac{\ell U_{0\ell}}{r} (1 - \theta^2) \tag{1}$$

where

$$F(\theta) = N_{Re} [1 - \theta^2], \quad N_{Re} = \frac{U_0 r}{\nu} = \frac{U_{0\ell} \ell}{\nu} \tag{2}$$

and U_0, the velocity along the axial streamline, $\theta = 0$, is inversely proportional to r. This is similar to the parabolic velocity distribution for plane Poiseuille flow. In our work, solutions of the convective diffusion equation were obtained only for values of N_{Re} and α for which Equation (1) is valid, and therefore the complex velocity profiles which may exist in Jeffery-Hamel flows were not considered in the present work. Calculations by Millsaps and Pohlhausen (*18*) indicate that Equation (1) is a reasonable approximation for

$$\left(\frac{4RU_{0\ell}}{\nu} \alpha\right) \lesssim 20$$

if $\alpha \leq 0.08$ rad. For $\alpha = 0.01$, the maximum value used in the present study, Equation (1) is probably a useful approximation as long as laminar flow is stable, say

$$\frac{4RU_{0\ell}}{\nu} \lesssim 2{,}000$$

Solution of the Convective Diffusion Equation

The convective diffusion equation, written in cylindrical coordinates for flow between nonparallel plates, as illustrated in Figure 1, is

$$\frac{\partial C^+}{\partial t} + U_0 \left(1 - \frac{\gamma^2}{\alpha^2}\right) \frac{\partial C^+}{\partial r} = \frac{D}{r} \frac{\partial}{\partial r} r \frac{\partial C^+}{\partial r} + \frac{D}{r^2} \frac{\partial^2 C^+}{\partial \gamma^2} \tag{3}$$

For the problem presently under consideration, the boundary conditions are

$$\begin{aligned} &C^+(0, r, \gamma) = 0, \quad r > \ell \\ &C^+(t, \ell, \gamma) = C_0^+, \quad t \geq 0 \\ &C^+(t, \infty, \gamma) = 0 \\ &\frac{\partial C^+}{\partial \gamma}(t, r, 0) = \frac{\partial C^+}{\partial \gamma}(t, r, \alpha) = 0 \end{aligned} \tag{4}$$

The physical conditions for which a step change inlet boundary condition is appropriate are discussed in reference *10*. If one introduces the dimensionless quantities

$$\tau = \frac{tD}{R^2}, \quad X = \frac{r}{RN_{Pe}} = \frac{rD}{R^2 U_{0\ell}}, \quad \theta = \frac{\gamma}{\alpha}, \quad C = \frac{C^+}{C_0} \tag{5}$$

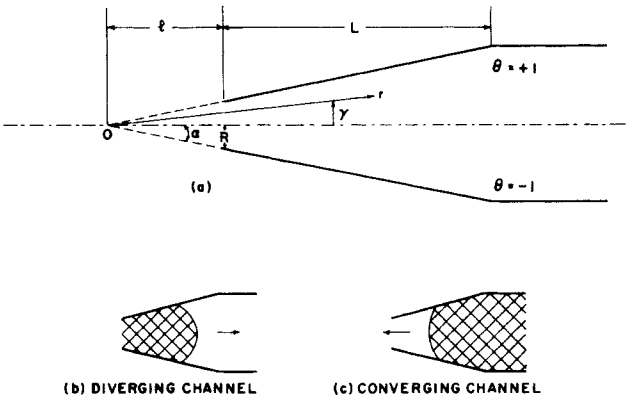

Fig. 1. Coordinate system for diverging channel.

Equation (3) reduces to

$$\frac{\partial C}{\partial \tau} + \frac{(1 - \theta^2)}{N_{Pe} \tan \alpha} \frac{1}{X} \frac{\partial C}{\partial X} = \frac{1}{N_{Pe}^2} \left[\frac{1}{X} \frac{\partial}{\partial X} X \frac{\partial C}{\partial X} + \frac{1}{\alpha^2 X^2} \frac{\partial^2 C}{\partial \theta^2}\right] \tag{6}$$

Solutions of Equation (6), which are valid for all values of time, were obtained by an alternating direction finite-difference method which is described by Guceri (*16*). These solutions are used to test the regions of applicability of the simplifications which can be made for certain values of the parameters. These simplifications will be discussed next.

Solutions for Large Peclet Number

Inspection of Equation (6) reveals that unlike the case of flow between parallel plates, in flows between nonparallel plates with finite α, the effect of having $N_{Pe} \longrightarrow \infty$ is to eliminate molecular diffusion, both axial and transverse, from the convective diffusion equation. Thus, in the event, $\alpha \neq 0$, $N_{Pe} \longrightarrow \infty$, Equation (6) reduces to

$$\frac{\partial C}{\partial \tau} + \frac{(1 - \theta^2)}{N_{Pe} \tan \alpha} \frac{1}{X} \frac{\partial C}{\partial X} = 0 \tag{7}$$

and the conditions are

$$\begin{aligned} &C(0, X) = 0 \\ &C\left(\tau, \frac{1}{N_{Pe} \tan \alpha}\right) = 1 \end{aligned} \tag{8}$$

Introducing the new variable

$$\xi_1 = \frac{z_1}{1 - \theta^2}, \quad z_1 = \frac{X^2 - X_e^2}{2X_e}, \quad X_e = (N_{Pe} \tan \alpha)^{-1} \tag{9}$$

we get

$$\frac{\partial C}{\partial \tau} + \frac{\partial C}{\partial \xi_1} = 0 \tag{10}$$

$$\begin{aligned} &C(0, \xi_1) = 0 \\ &C(\tau, 0) = 1 \end{aligned} \tag{11}$$

By using the LaPlace transform, it is easy to show that

$$C = \begin{cases} 0 \Longrightarrow \theta > \sqrt{1 - \dfrac{z_1}{\tau}} \\ 1 \Longrightarrow 1 > \sqrt{1 - \dfrac{z_1}{\tau}} > \theta \end{cases} \tag{12}$$

and therefore

$$C_m = \sqrt{1 - \frac{z_1}{\tau}} = \sqrt{1 - \left(\frac{r^2}{\ell^2} - 1\right) \frac{\ell}{2tU_0\ell}} \tag{13}$$

For parallel plates, this reduces to

$$C_m = \sqrt{1 - \frac{x}{tU_0^+}} \tag{14}$$

A Proposed Dispersion Model Solution

In the past, dispersion models have been proposed and have proved to be valid under limited conditions to describe the behavior of systems with parallel walls. No comparable models have been proposed for systems with nonparallel walls, and thus we propose a new one for Jeffery-Hamel flow in diverging channels. To do this, we assume that the transport of material by convection $U_m C_b^+$ across any surface at a constant value of r can be described by

$$U_m C_b^+ = U_m C_m^+ - k^+ \frac{\partial C_m^+}{\partial r}$$

Integration of Equation (3) from 0 to α shows that this basic assumption leads to the proposed dispersion model which is

$$\frac{\partial C_m^+}{\partial t} + \frac{2}{3} U_0 \frac{\partial C_m^+}{\partial r} = \frac{K^+}{r} \frac{\partial}{\partial r} r \frac{\partial C_m^+}{\partial r} \tag{15}$$

where the mean velocity $U_m = \frac{2}{3} U_0$, and which, in dimensionless form, is

$$\frac{\partial C_m}{\partial \tau} + \frac{2}{3N_{Pe} \tan \alpha} \frac{1}{X} \frac{\partial C_m}{\partial X} = \frac{K}{N_{Pe}^2} \frac{1}{X} \frac{\partial}{\partial X} X \frac{\partial C_m}{\partial X} \tag{16}$$

The Large Time Solution

Several limiting solutions of Equation (16) of interest can be found relatively easily. First, we found that a remarkably simple solution valid for large values of τ exists. To find this solution, let

$$X_p = \frac{\ell}{2U_0 t} \left(\frac{r^2}{\ell^2} - 1\right) t^{-1} \tag{17}$$

and in (τ, X_p) coordinates, Equation (16) becomes

$$\tau \frac{\partial C_m}{\partial \tau} = \left(\frac{2K \tan \alpha}{N_{Pe}} + X_p - \frac{2}{3}\right) \frac{\partial C_m}{\partial X_p} = \frac{2K \tan \alpha}{N_{Pe}} \left(X_p + \frac{1}{2N_{Pe} \tan \alpha \, \tau}\right) \frac{\partial^2 C_m}{\partial X_p^2} \tag{18}$$

If we expand C_m as

$$C_m = C_{m_0}(X_p) + \sum_{n=1}^{\infty} C_{m_n}(X_p) \tau^{-n} \tag{19}$$

we find that $C_{m_0}(X_p)$, the solution valid for large τ, is given by the solution of

$$\frac{2K \tan \alpha}{N_{Pe}} X_p \frac{d^2 C_{m_0}}{dX_p^2} + \left(\frac{2}{3} - X_p\right) \frac{dC_{m_0}}{dX_p} = 0 \tag{20}$$

The solution to Equation (20) is given as an incomplete gamma function in the form

$$C_{m_0} = 1 - \frac{\int_0^{\beta_1} \varepsilon^{(\phi-1)} e^{-\varepsilon} d\varepsilon}{\int_0^{\infty} \varepsilon^{(\phi-1)} e^{-\varepsilon} d\varepsilon} = \frac{\Gamma(\beta_1, \phi)}{\Gamma(\phi)} \tag{21}$$

where

$$\beta_1 = \frac{N_{Pe}}{2K \tan \alpha} X_p, \quad \phi = \frac{N_{Pe}}{3K \tan \alpha}$$

When ϕ is large, say greater than 75, the incomplete gamma function can be evaluated much more conveniently as an error function, and then C_{m_0} is given by

$$C_{m_0} = 1 - \frac{1}{\sqrt{2\pi}} \int_{-\infty}^{\beta_1 - \phi/\sqrt{\phi}} e^{-\varepsilon^2/2} d\varepsilon = 1 - \frac{1}{2}\left[1 + \operatorname{erf}\left(\frac{\beta_1 - \phi}{\sqrt{2\phi}}\right)\right] \tag{21a}$$

The Solution for Small Angles of Divergence

Another solution, which enables one to obtain an expression for K for small values of α, can be found in the following manner. If one defines a new variable ξ such that

$$\xi = \ln \frac{z}{z_0} = \ln \frac{r^2}{\ell^2} \tag{22}$$

where

$$z = \frac{X^2}{2} \quad \text{and} \quad z_0 = \frac{1}{2N_{Pe}^2 \tan^2 \alpha} \tag{23}$$

then Equations (6) and (16) become

$$z_0 e^{\xi} \frac{\partial C}{\partial \tau} + \frac{(1 - \theta^2)}{N_{Pe} \tan \alpha} \frac{\partial C}{\partial \xi} = \frac{1}{N_{Pe}^2} \left[2 \frac{\partial^2 C}{\partial \xi^2} + \frac{1}{2\alpha^2} \frac{\partial^2 C}{\partial \theta^2}\right] \tag{24}$$

and

$$z_0 e^{\xi} \frac{\partial C_m}{\partial \tau} + \frac{2}{3N_{Pe} \tan \alpha} \frac{\partial C_m}{\partial \xi} = \frac{2K}{N_{Pe}^2} \frac{\partial^2 C_m}{\partial \xi^2} \tag{25}$$

In the limit of $\alpha \longrightarrow 0$, $z \longrightarrow z_0$, and considerable simplification is introduced if we consider only small values of α such that z is not much different from z_0 and e^{ξ} can be approximated by 1. In this case, Equations (24) and (25) reduce to

$$\frac{\partial C}{\partial \bar{\tau}} + \frac{1}{N_{Pe} \tan \alpha} \left(\frac{1}{3} - \theta^2\right) \frac{\partial C}{\partial \zeta} = \frac{1}{N_{Pe}^2} \left[2 \frac{\partial^2 C}{\partial \zeta^2} + \frac{1}{2\alpha^2} \frac{\partial^2 C}{\partial \theta^2}\right] \tag{26}$$

and

$$\frac{\partial C_m}{\partial \bar{\tau}} = \frac{2K}{N_{Pe}^2} \frac{\partial^2 C_m}{\partial \zeta^2} \tag{27}$$

where

$$\bar{\tau} = \frac{\tau}{z_0}, \quad \zeta = \xi - \frac{2\tau}{3N_{Pe} \tan \alpha} \tag{28}$$

so that

$$C_m = \frac{1}{2}\left\{\operatorname{erfc} \frac{X_p - \frac{2}{3}}{\sqrt{4K/\tau N_{Pe}^2}} + \exp\left[\frac{4\tau N_{Pe}^2}{3K} X_p\right] \operatorname{erfc}\left[\frac{X_p + \frac{2}{3}}{\sqrt{4K/\tau N_{Pe}^2}}\right]\right. \tag{29}$$

It is clear from reference *14a* that an exact solution of Equation (26) would involve an infinite set of coefficients and a dispersion model with higher order derivatives with respect to ζ than Equation (27) contains. However, in the present work we are concerned only with obtaining an approximate solution. Reference *13* suggests that a useful

form of solution of Equation (26) is

$$C = C_m + \sum_{k=1}^{\infty} f_k(\bar{\tau}, \theta) \frac{\partial^k C_m}{\partial \zeta^k} \tag{30}$$

and substituting Equation (30) in Equation (26), also using Equation (27) to replace the time derivatives, we get

$$\left[\frac{\partial f_1}{\partial \bar{\tau}} + \frac{(\frac{1}{3} - \theta^2)}{N_{Pe} \tan \alpha} - \frac{1}{2\alpha^2 N_{Pe}^2} \frac{\partial^2 f_1}{\partial \theta^2}\right] \frac{\partial C_m}{\partial \zeta} + \left[\frac{\partial f_2}{\partial \bar{\tau}} + \frac{(\frac{1}{3} - \theta^2)}{N_{Pe} \tan \alpha} f_1 + \frac{2}{N_{Pe}^2}(K-1) - \frac{1}{2\alpha^2 N_{Pe}^2} \frac{\partial^2 f_2}{\partial \theta^2}\right] \frac{\partial^2 C_m}{\partial \zeta^2} + \sum_{k=1}^{\infty} \left[\frac{\partial f_{k+2}}{\partial \bar{\tau}} + \frac{(\frac{1}{3} - \theta^2)}{N_{Pe} \tan \alpha} f_{k+1} + \frac{2}{N_{Pe}^2}(K-1) f_k - \frac{1}{2\alpha^2 N_{Pe}^2} \frac{\partial^2 f_{k+2}}{\partial \theta^2}\right] \frac{\partial^{k+2} C_m}{\partial \zeta^{k+2}} = 0 \tag{31}$$

If one lets $f_1 = f_{1s}(\theta) + f_{1t}(\bar{\tau}, \theta)$ and equates the coefficients of first-order derivatives, the following equation defines f_{1s}, which is the part of f_1 that remains finite as $\tau \to \infty$:

$$\frac{d^2 f_{1s}}{d\theta^2} = \frac{2\alpha^2 N_{Pe}}{\tan \alpha}\left(\frac{1}{3} - \theta^2\right) \tag{32}$$

The boundary conditions, derived from Equations (4) and (30), are

$$\left.\begin{aligned} \frac{df_{1s}}{d\theta}(0) &= \frac{df_{1s}}{d\theta}(1) = 0 \\ \int_0^1 f_{1s}\, d\theta &= 0 \end{aligned}\right\} \tag{33}$$

so that f_{1s} is

$$f_{1s} = \frac{2\alpha^2 N_{Pe}}{\tan \alpha}\left(\frac{\theta^2}{6} - \frac{\theta^4}{12} - \frac{7}{180}\right) \tag{34}$$

Similarly, equating the coefficients of second-order derivatives of C_m with respect to ζ in Equation (31), we get

$$\frac{d^2 f_{2s}}{d\theta^2} = 2\alpha^2 N_{Pe}^2 \left[\frac{2K}{N_{Pe}^2} - \frac{2}{N_{Pe}^2} + \frac{1}{N_{Pe} \tan \alpha}\left(\frac{1}{3} - \theta^2\right) f_{1s}\right] \tag{35}$$

and the boundary conditions are

$$\left.\begin{aligned} \frac{df_{2s}}{d\theta}(0) &= \frac{df_{2s}}{d\theta}(1) = 0 \\ \int_0^1 f_{2s}\, d\theta &= 0 \end{aligned}\right\} \tag{36}$$

By integrating once, Equation (35) becomes

$$\frac{df_{2s}}{d\theta} = (4\alpha^2 K - 4\alpha^2)\,\theta + \left(\frac{2\alpha^2 N_{Pe}}{\tan \alpha}\right)^2 \left(-\frac{7}{540}\,\theta + \frac{17}{540}\,\theta^3 - \frac{7}{180}\,\theta^5 + \frac{1}{84}\,\theta^7\right) \tag{37}$$

and therefore the boundary condition $\frac{df_{2s}}{d\theta}(1) = 0$ requires K to be

$$K = 1 + \frac{8}{945}\frac{\alpha^2 N_{Pe}^2}{\tan^2 \alpha} \tag{38}$$

and f_{2s} is

$$f_{2s} = 2\alpha^2(K-1)\left(\theta^2 - \frac{1}{3}\right) + \left(\frac{\alpha^2 N_{Pe}}{\tan \alpha}\right)\left[\frac{1}{168}\,\theta^8 - \frac{7}{270}\,\theta^6 + \frac{17}{540}\,\theta^4 - \frac{7}{270}\,\theta^2 + \frac{611}{113{,}400}\right] \tag{39}$$

It is worth noting that K, described by Equation (38), reduces to

$$K = 1 + \frac{8N_{Pe}^2}{945} \tag{40}$$

as $\alpha \to 0$, which is the same as Philip (*19*) found for parallel plates. It is also worth noting that one can obtain Equation (38) by assuming $\partial C/\partial \tau = \partial C_m/\partial \tau$ in Equation (24), rather than $z \to z_0$.

DISCUSSION OF RESULTS

A major aspect of this work is the extensive numerical solutions of Equation (6) for diverging channels which were obtained by an alternating direction implicit finite-difference method for numerous values of the parameters up to the approximate values of τ shown in Table 1. The α values were chosen such that flow separation did not occur, and therefore to be conservative the solutions were obtained for small values of α up to 0.01 rad. These numerical experiments, which revealed some rather surprising information concerning the role of molecular diffusion in diverging channels, were performed primarily to determine the ranges of the parameters in which the various transport mechanisms (molecular diffusion and convection in the direction of flow and transverse molecular diffusion) are dominant, and the ranges in which the dispersion model and large N_{Pe} solutions apply for flow in channels with diverging walls. The finite-difference analysis is described in detail in reference *16*.

TABLE 1. MAXIMUM VALUE OF DIMENSIONLESS TIME τ UP TO WHICH EXACT SOLUTIONS ARE AVAILABLE (α GIVEN IN RADIANS)

N_{Pe} \ α	0.01 radians	0.001	0.0001	0
10	—	—	—	15
25	22	—	—	23
50	23	23	23	23
100	24	—	—	
200	175	25	25	24
400	167	—	—	
1,000	1.8	—	—	4
10,000	110	—	—	

Parallel Plate Results

First we consider the case of parallel plates ($\alpha = 0$), since the regions of applicability of pure convection and dispersion model solutions for this system, unlike tubes, have not been discussed previously in the literature. An approximate map of the regions in which the various solutions are valid is given in Figure 2. In this case, where $\alpha = 0$, in contrast to the case of nonparallel plates, the dispersion model given by

$$C_m = -\left[\operatorname{erfc}\left(\frac{X/\tau - \frac{2}{3}}{\frac{2}{N_{Pe}\tau}\sqrt{K\tau}}\right) + \exp\left(\frac{2XN_{Pe}^2}{3K}\right)\operatorname{erfc}\left(\frac{X/\tau + \frac{2}{3}}{\frac{2}{N_{Pe}\tau}\sqrt{K\tau}}\right)\right] \tag{41}$$

with K given by Equation (38), is exact as $\tau \longrightarrow \infty$. For most practical purposes Equation (41) is accurate enough in the region shown in Figure 2. Also shown is the region where the pure convection solution, given by Equation (14), is valid.

The criterion used to obtain the results in Figure 2 is that the numerical results agree with Equation (41) within at least 5% everywhere between the points having an average concentration of approximately 5 and 98%. As one would expect, the results for parallel plates are qualitatively the same as those for flow in tubes.

A quantity of significant practical interest is the length of the mixing zone which is a measure of the extent of interaction between the displaced and displacing fluids. In the present study, L_m is the dimensionless length ΔX over which the average concentration changes from 0.9 to 0.1. In Figure 3 it is seen that the mixing length increases with τ and also, as expected, as the Peclet number decreases.

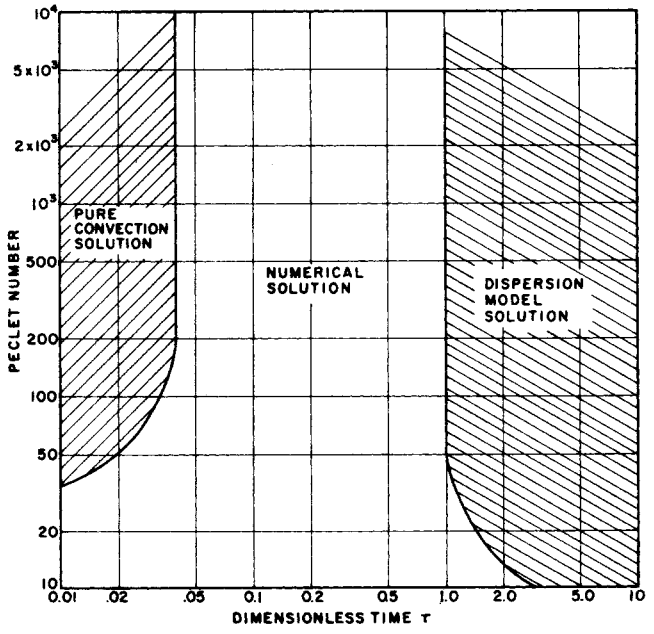

Fig. 2. Map of regions of applicability of the pure convection and dispersion model solutions. For the intervening region only the numerical solution is known.

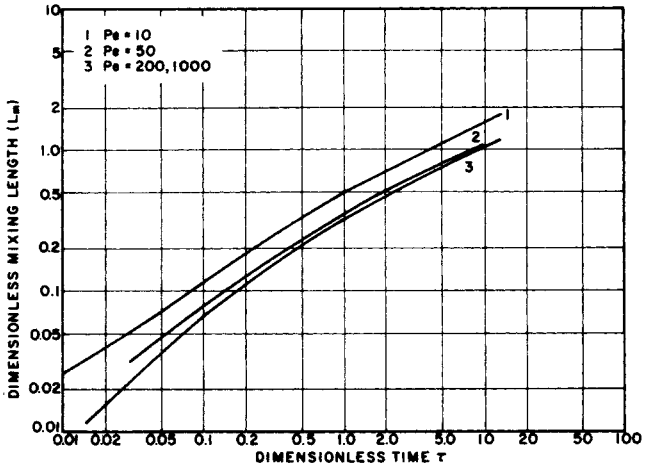

Fig. 3. Mixing length for concentration C_m between 0.1 and 0.9 as a function of τ and N_{Pe}.

Diverging Channel Results

Examination of the numerical solutions of Equation (6) for the values of the parameters listed in Table 1 reveals several interesting aspects of the behavior of the average concentration distribution. First, with $\alpha = 0.01$, if αN_{Pe}^2 is greater than 10^6, the pure convection solution, Equation (13), is valid for all values of τ. Second, for large values of τ, the average concentration profiles become functions of $X_p = \left(\frac{r^2}{\ell^2} - 1\right) \frac{\ell}{2U_{0\ell}t}$ only, as required by Equation (21). Third, for small values of α and N_{Pe} the small α model, Equation (29), is convenient because the numerical results show that it requires very large values of τ for the average concentration profiles to become functions of X_p only, in which case Equation (21) would apply.

One of the most striking results of this study is that the pure convection solution is valid for dispersion in flow between nonparallel walls for much larger values of τ than for parallel plate or capillary systems. For example, with $\alpha = 0.01$ and Peclet numbers of 10^4 or greater, the average concentration distribution is given by Equation (13) for all values of τ of practical interest. This is illustrated in Figure 4 which shows that the concentration distribution is given by Equation (13) up to $\tau = 110$ which is the maximum value of τ for which numerical solutions of Equation (6) were obtained for $N_{Pe} = 10^4$, $\alpha = 0.01$. The implication is that both transverse and axial molecular diffusion play a minor role in dispersion in diverging channels at high Peclet number. This result is in contradistinction to that obtained in parallel plate systems, where axial diffusion becomes negligible when the Peclet number exceeds 100 but

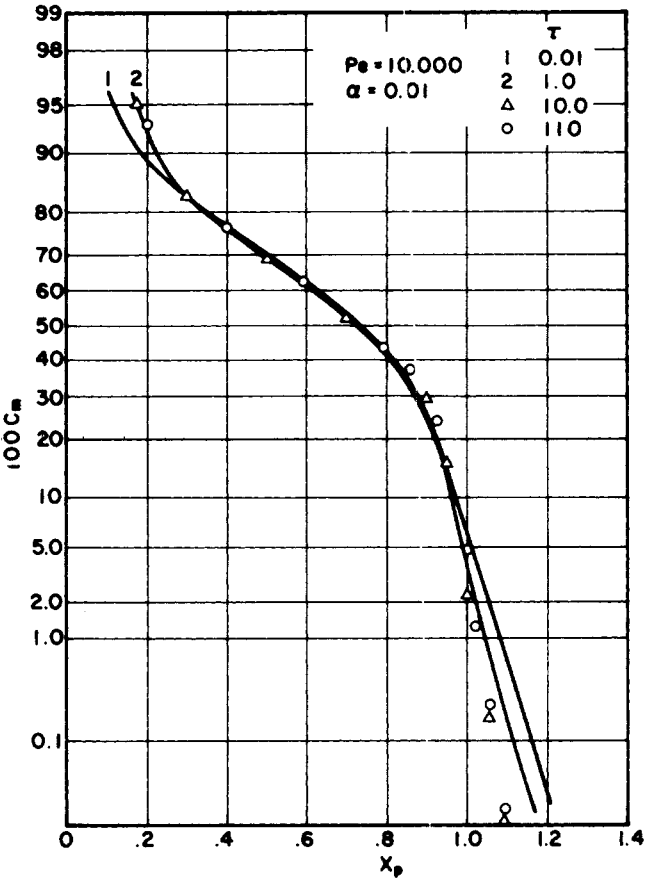

Fig. 4. Numerical results for $\alpha = 0.01$ and $N_{Pe} = 10^4$. These results agree well with pure convection solution for all τ of practical interest.

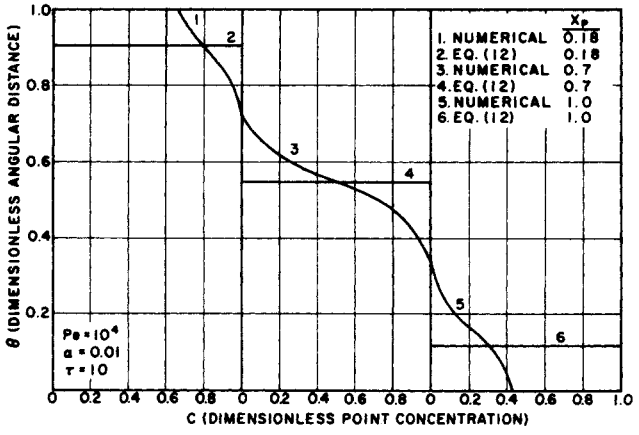

Fig. 5. Comparison of numerical results for local concentration distribution with pure convection solution.

transverse diffusion remains significant for all values of the Peclet number. The local concentration distributions shown in Figure 5 for several axial positions illustrate that the main effect of molecular diffusion is to round off the pure convection distribution in the regions where maximum concentration gradients exist.

For smaller values of Peclet number, the pure convection solution applies only at small values of τ as is the case with parallel wall systems. As the Peclet number is decreased further, axial molecular diffusion becomes significant as indicated by the concentration distribution for $N_{Pe} = 50$ in Figure 6.

The fact that the pure convection solution is dominant for longer time in diverging channels than in tubes or parallel plates can be understood mathematically by noting that $1/N_{Pe}^2$ multiplies both the axial and radial molecular diffusion terms in Equation (6). However, as $\alpha \longrightarrow 0$, Equation (6) degenerates to

$$\frac{\partial C}{\partial \tau} + (1 - y^2)\frac{\partial C}{\partial x_1} = \frac{1}{N_{Pe}^2}\frac{\partial^2 C}{\partial x_1^2} + \frac{\partial^2 C}{\partial y^2} \qquad (42)$$

and $1/N_{Pe}^2$ multiplies only the axial diffusion term. Therefore, as $N_{Pe} \longrightarrow \infty$, only the axial diffusion term $\frac{1}{N_{Pe}^2}\frac{\partial^2 C}{\partial x_1^2}$ vanishes if $\alpha = 0$, but for $\alpha \neq 0$, one sees that the entire right-hand side of Equation (6) vanishes as shown in Equation (7). Consequently, the proper limit for $N_{Pe} \longrightarrow \infty$ and $\alpha \longrightarrow 0$ is Equation (42) without the axial diffusion term.

Some physical insight into the reasons for this behavior can be gained by observing the behavior of the velocity distribution as illustrated in Figure 7. Note that the velocity profiles become flatter as one moves downstream, and this reduces the surface area across which a steep radial concentration gradient exists and therefore decreases the effect of transverse molecular diffusion. As the velocity gets flatter, in the limit, the surface area across which molecular diffusion occurs degenerates to a plane, the outer normal of which is parallel to the direction of main flow. In contrast, with tubes or parallel plates, the velocity profile is invariant with axial position, and, as time increases, convection creates an increasingly larger paraboloid surface across which transverse concentration gradients are very large.

As predicted by Equation (21), the average concentration distributions shown in Figure 8 are functions of X_p only, providing τ is large enough. Apparently, in the range of N_{Pe} equal 50 to 10^3, transverse diffusion is not sufficiently intense to counteract the axial convection effect to the extent it does in Taylor type of diffusion, but it is important enough to modify significantly the distribution from that which would occur if forced convection were the only mechanism operating. That is, only for $N_{Pe} = 25$ does the average concentration distribution become a straight line on probability coordinates, a characteristic of Taylor type of diffusion. Apparently this occurs when $\alpha N_{Pe} \lesssim 0.5$.

At $N_{Pe} = 25$, 50, 100, and 200 and $\alpha = 0.01$, the numerical results for the average concentration distribution are in rather good agreement with Equation (21) if K is given by Equation (38). However, comparison of the numerical results with the dispersion model approximate solutions,

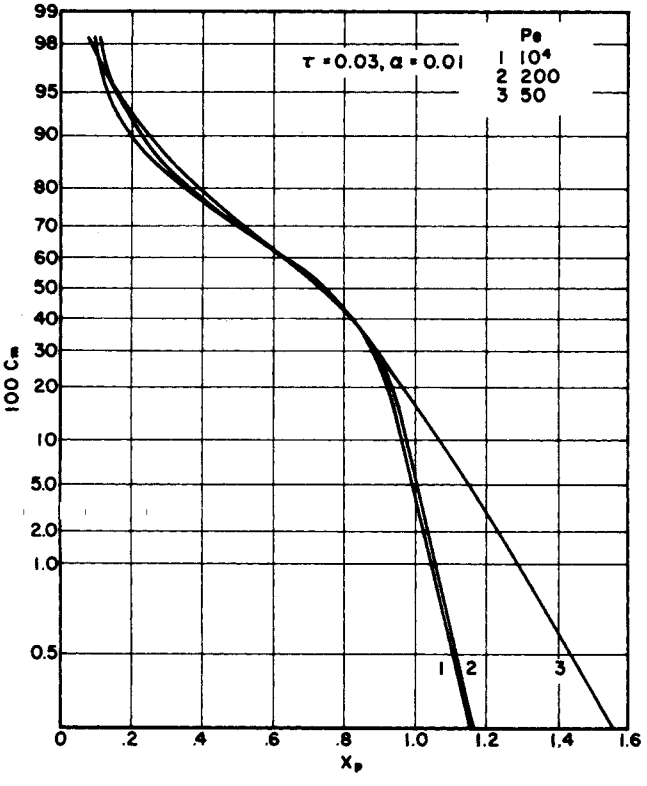

Fig. 6. Effect of axial diffusion on average concentration distribution for small τ. Note axial diffusion significant only for curve 3.

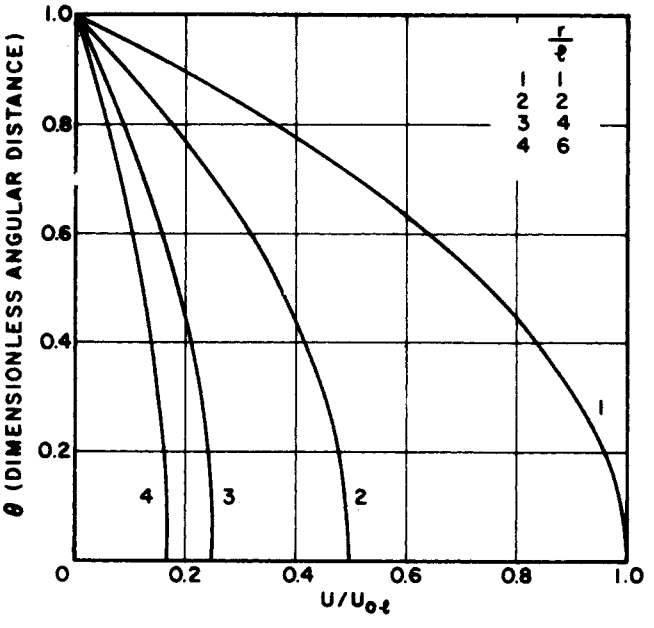

Fig. 7. Local velocity distribution for diverging channels for several values of r/ℓ. Note flattening of distribution with increasing r/ℓ.

Equations (21) and (29), shows that Equation (38) is an oversimplification of the dependence of K on α and N_{Pe}. For example, Equation (38) predicts that the dispersion coefficient for dispersion between diverging plates is always equal to or less than that for flow between parallel plates. However, a comparison of the results of Equation (21) with the numerical results given in Figure 8 reveals for $\alpha = 0.01$ that this is not necessarily true. For example, agreement between the numerical results and Equation (21) is improved for $N_{Pe} = 25$ and 400 if K is respectively greater than and less than that predicted by Equation (38).

Comparison of the average concentration distributions predicted by Equation (21) with the numerical data in Figure 8 for $N_{Pe} \gtrsim 400$ indicates that the dispersion model solution does not change rapidly enough in the range $0.8 \leq X_p \leq 1.0$. This is apparently the region in which the transition from dispersion model to pure convection behavior occurs. Very rapid changes in the average concentration distribution are characteristic of pure convection systems, and this is one of the reasons why it is difficult to obtain accurate finite difference solutions of such systems.

Figure 9 illustrates the way concentration profiles change with τ when C_m is plotted versus X_p for $N_{Pe} = 400$ and $\alpha = 0.01$. The profiles change from the pure convection solution, which is invariant for small values of τ, to the distribution, which is invariant for large values of τ. Figure 10 also illustrates how the profiles change with τ, but, in this case, with the exception of $\tau = 1.0$, the profiles are all straight lines.

The magnitude of τ necessary to have the profiles become functions of X_p only seems to increase as αN_{Pe} decreases; $\tau \simeq 1.5$ is required for $\alpha = 0.01$ and $N_{Pe} = 10^3$, whereas $\tau \simeq 15$ is required for $\alpha = 0.01$ and $N_{Pe} = 50$. For $\alpha = 0.001$ if $N_{Pe} = 5$, the value of τ required is signifi-

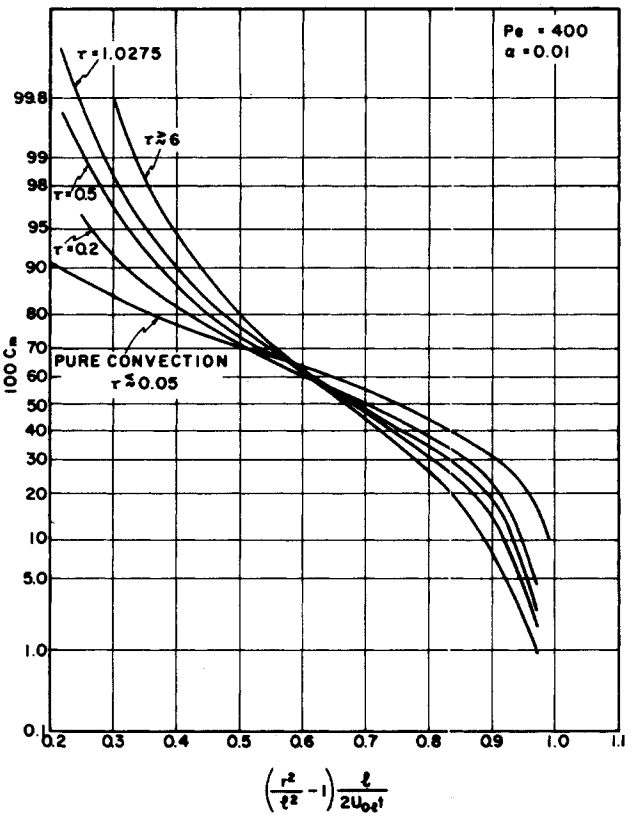

Fig. 9. Numerical results demonstrating variation of average concentration distribution with τ. Results independent of τ above $\tau \simeq 6$.

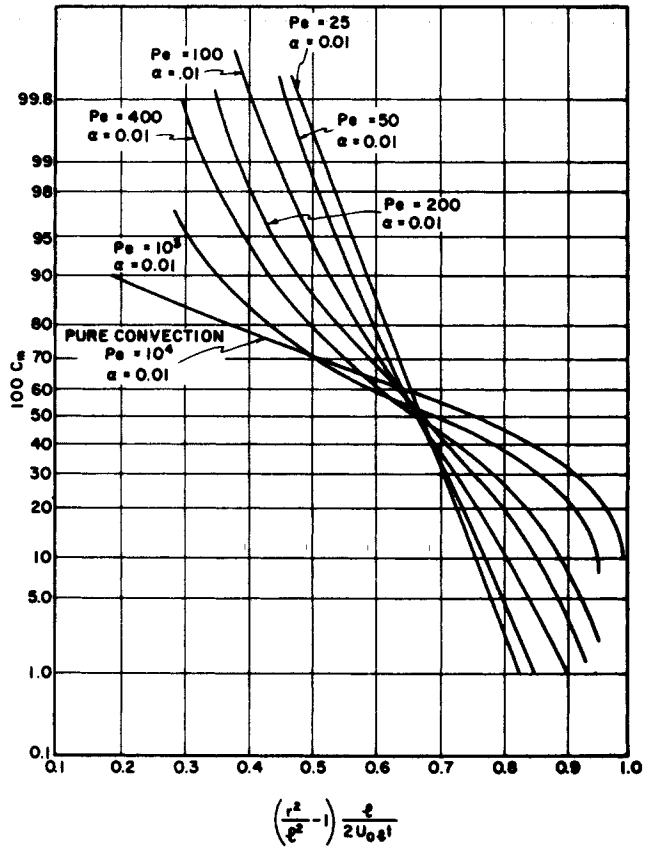

Fig. 8. τ independent numerical results for average concentration distributions at large values of τ.

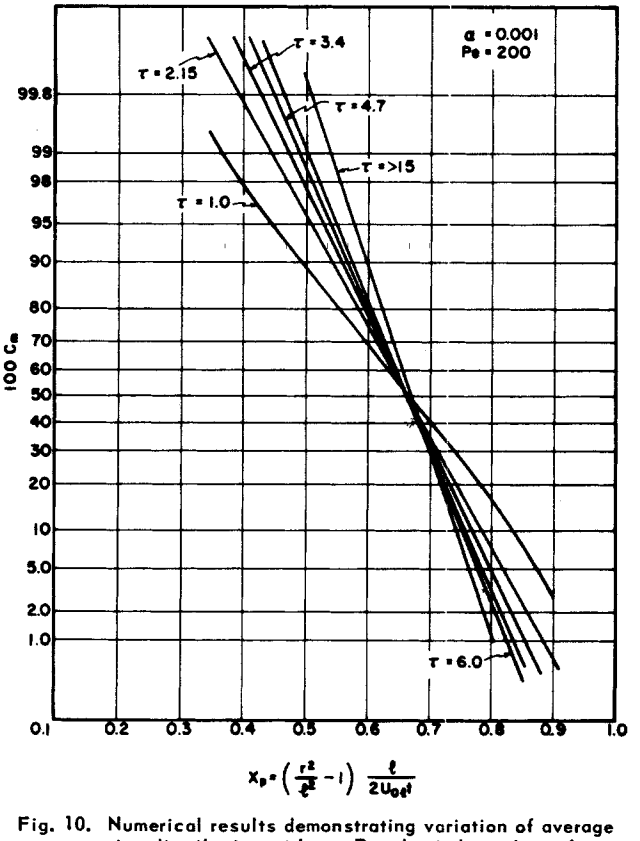

Fig. 10. Numerical results demonstrating variation of average concentration distribution with τ. Results independent of τ above $\tau \simeq 15$.

cantly greater than 20, but for $N_{Pe} = 200$, $\tau \simeq 15$ is sufficient. This implies that the practical value of Equation (21) is limited when α is very small because such large values of τ are required. In these cases, Equation (29) is more useful.

CONCLUSIONS

Miscible displacement in systems with diverging boundaries is considerably more complicated than in parallel wall systems. This makes the computer time requirements very large if one wishes to do a comprehensive numerical study of the problem. Nevertheless, some reasonably general statements about the dispersion process occurring in such systems can be made on the basis of the present study.

Three characteristics of the solutions of the convective diffusion equation, Equation (3), for flow in diverging channels seem particularly interesting.

1. Unlike parallel plate systems, in diverging channels, for larger values of Peclet number and α, say greater than 10^4 and 0.01, respectively, the average concentration distribution is accurately described by the pure convection solution, Equation (13). This is true for all values of τ of practical interest. In parallel plate systems, the dispersion model applies for arbitrarily large Peclet numbers, providing τ is greater than about 1.0.

2. After a certain dimensionless time τ has elapsed, the average concentration distribution calculated from Equation (3) becomes a function of X_p only, as predicted by Equation (21). This behavior simplifies the determination of the region of applicability of the dispersion model given by Equation (15) and suggests that this proposed model is valid.

3. The Peclet number range of applicability of the dispersion model varies with α and increases to higher N_{Pe} as α decreases. For example, with $\alpha = 0.01$, the dispersion model applies for $N_{Pe} \lesssim 200$, whereas for $\alpha = 0$, it applies for all values of N_{Pe} if τ is sufficiently large.

ACKNOWLEDGMENT

This work was supported in part by the Office of Saline Water, U. S. Department of Interior.

NOTATION

C = dimensionless point concentration, C^+/C_0^+
C^+ = point concentration
C_b^+ = bulk mean concentration $= \dfrac{1}{U_m \alpha} \displaystyle\int_0^\alpha U C^+(t, r, \gamma)\, d\gamma$
C_0^+ = initial concentration of the solute, at $X = 0$
C_m = dimensionless average concentration, C_m^+/C_0^+
C_m^+ = average concentration $= \dfrac{1}{\alpha} \displaystyle\int_0^\alpha C^+(t, r, \gamma)\, d\gamma$
D = molecular diffusion coefficient
$f_k(\tau, \theta)$ = defined by Equation (30)
k^+ = dispersion coefficient due to axial convection and transverse molecular diffusion
K^+ = total dispersion coefficient including axial molecular diffusion, $k^+ + D$
K = dimensionless dispersion coefficient, K^+/D
ℓ = entrance length
L_m = mixing length through which significant changes in concentration occur
N_{Pe} = Peclet number, $RU_{0\ell}/D$ (or $U_0^+ R^+/D$ for parallel plates)
N_{Re} = Reynolds number, $U_0 r/\nu$
r = radial distance
R = half width of the parallel plate duct at the channel entrance
R^+ = half width of the parallel plate duct
t = time through which the solute disperses
U = velocity of fluid
U_m = average or mean velocity
U_0 = velocity in the center of the channel
U_0^+ = velocity in the center of the parallel plate duct
$U_{0\ell}$ = maximum velocity at the entrance of the channel
x = axial coordinate in parallel plate geometry
X = dimensionless axial coordinate $\dfrac{xD}{R^{+2}U_0^+}$ for parallel plates, $\dfrac{rD}{R^2 U_{0\ell}}$ for nonparallel plates
X_p = dimensionless axial coordinate, $\left(\dfrac{r^2}{\ell^2} - 1\right) \dfrac{\ell}{2tU_{0\ell}}$
X_e = dimensionless entrance, length, $\dfrac{1}{N_{Pe} \tan \alpha} = \dfrac{\ell D}{U_{0\ell} R^2}$
z = dimensionless axial coordinate, $X^2/2$
z_0 = dimensionless entrance length, $X_e^2/2$.
z_1 = dimensionless axial coordinate defined by Equation (9)

Greek Letters

α = angle of divergence
γ = angular coordinate, Figure 1
θ = dimensionless angular coordinate, γ/α
ν = kinematic viscosity
τ = dimensionless time, Dt/R^2 (or Dt/R^{+2} for parallel plates)
$\bar{\tau}$ = dimensionless time, τ/z_0
ξ = dimensionless axial coordinate, $\ln z/z_0$
$\xi_1 = \dfrac{z_1}{1 - \theta^2}$
ζ = dimensionless axial coordinate, $\xi - \dfrac{2\tau}{3N_{Pe} \tan \alpha}$

LITERATURE CITED

1. Ananthakrishnan, V., W. N. Gill, and A. J. Barduhn, *AIChE J.*, **11**, 1063 (1965).
2. Aris, Rutherford, *Proc. Roy. Soc.*, **235A**, 67 (1956).
3. *Ibid.*, **252A**, 538 (1959).
4. *Ibid.*, **259A**, 370 (1960).
5. Bailey, H. R., and W. B. Gogarty, *ibid.*, 352.
6. Bournia, A., J. Coull, and G. Houghton, *ibid.*, **261A**, 227 (1961).
7. Carrier, G. F., *Quart. Appl. Math.*, **14**, 108 (1956).
8. Eagles, P. M., *J. Fluid Mech.*, **24**, 191 (1966).
9. Erdogan, M. E., and P. C. Chatwin, *ibid.*, **29**, 465 (1967).
10. Gill, W. N., and V. Ananthakrishnan, *AIChE J.*, **12**, 906 (1966).
11. *Ibid.*, **13**, 801 (1967).
12. Gill, W. N., *Chem. Eng. Sci.*, **22**, 1013 (1967).
13. ———, *Proc. Roy. Soc.*, **298**, 335 (1967).
14. Gill, W. N., *AIChE J.*, **15**, 745 (1969).
14a. Gill, W. N., and R. Sankarasubramanian, *Proc. Roy. Soc.*, **A316**, 341 (1970).
15. Goldstein, S., *J. Fluid Mech.*, **21**, 33 (1965).
16. Güceri. Ülkü, Masters thesis, Clarkson College, Potsdam, N. Y. (1968).
17. Jeffery, G. B., *Phil. Mag.*, **29**, 455 (1915).
18. Millsaps, K., and K. Polhausen, *J. Aeron. Sci.*, **20**, 187 (1953).
18a. Nunge, R. J., T. S. Lin, and W. N. Gill, "Laminar Dispersion in Curved Tubes and Channels," Reprint 49f, 62nd Annual Meeting, AIChE, Washington, D.C. (1969).
19. Philip, J. R., *Australian J. Phys.*, **16**, 287 (1963).
20. Reejhsinghani, N. S., W. N. Gill, and A. J. Barduhn, *AIChE J.*, **12**, 916 (1966).
21. ———, *Ibid.*, *AIChE J.*, **14**, 100 (1968).
22. Rosenhead, L., *Proc. Roy. Soc. (London)*, **175**, 436 (1940).
23. Taylor, G. I., *Proc. Roy. Soc.*, **219A**, 186 (1953).
24. *Ibid.*, **223A**, 446 (1954).

Manuscript received February 28, 1969; revision received June 2, 1969; paper accepted June 4, 1969.